Electronic Supplementary Material (ESI) for Journal of Materials Chemistry C.

SUPPLEMENTARY INFORMATION

Conductive, self-Healable and reusable poly(3,4-ethylenedioxythiophene)-based hydrogels for highly sensitive pressure arrays

Ismael Babeli,[a,◊] Guillem Ruano,[a,◊] Jordi Casanovas,[b] Maria-Pau Ginebra,[c,d,e] Jose García-Torres[c,d,*] and Carlos Alemán[a,d,e,*]

[a] *Departament d'Enginyeria Química, EEBE, Universitat Politècnica de Catalunya, C/ Eduard Maristany, 10-14, 08019, Barcelona, Spain*

[b] *Departament de Química, Escola Politècnica Superior, Universitat de Lleida, c/Jaume II no. 69, Lleida E-25001, Spain*

[c] *Biomaterials, Biomechanics and Tissue Engineering Group, Department of Materials Science and Metallurgical Engineering, Universitat Politècnica de Catalunya (UPC), 08930 Barcelona, Spain*

[d] *Barcelona Research Center in Multiscale Science and Engineering, Universitat Politècnica de Catalunya, 08930 Barcelona, Spain*

[e] *Institute for Bioengineering of Catalonia (IBEC), Barcelona Institute of Science and Technology (BIST), Baldiri Reixac 10-12, 08028 Barcelona Spain*

[◊] These authors contributed equally to this work

[*] jose.manuel.garcia-torres@upc.edu and carlos.aleman@upc.edu

EXPERIMENTAL SECTION

Theoretical calculations

The strength of PEDOT···PSS and PEDOT···alginate interaction was examined using Density Functional Theory (DFT) calculations, which were performed using the Gaussian 09 computer package.[S1] The geometries of the different investigated model complexes were fully optimized with the M06L[S2,S3] functional, which was developed by Zhao and Truhlar to account for dispersion, combined with the 6-31G(d,p) basis set. Geometry optimizations were performed in vacuum and in water (ε= 32.6), which was described through a simple Self Consistent Reaction Field (SCRF) method. More specifically, the Polarizable Continuum Model[S4,S5] (PCM) was used in the framework of the M06L/6-31G(d,p) level to represent bulk solvent effects. No symmetry constraints were used in the geometry optimizations.

Preparation of hydrogels.

PEDOT:PSS 1.3 wt. % dispersion in H_2O, Alginic acid (AA) from Macrocystis pyrifera (61% mannuronic acid and 39% guluronic acid; M_W= 240 kDa) were purchased from Sigma-Aldrich, while $CaCl_2$ was purchased from Scharlab.

The 1.3 wt% and 3.9 wt% AA solutions were prepared by dissolving the biopolymer in deionized water at 50 ºC with vigorous stirring for 1 h. Then, equal volumes of the 1.3 wt% PEDOT:PSS dispersion and each of these AA solutions were mixed at room temperature with vigorous stirring for 20 min. Hereafter, the mixtures coming from 1.3 wt% and 3.9 wt% AA solutions are denoted 1:1 PEDOT:PSS/AA and 1:3 PEDOT:PSS/AA. Also, the 3:1 PEDOT:PSS/AA mixture was prepared using 1.3 wt% AA and increasing three times the volume of PEDOT:PSS with respect to that of AA. Hydrogels were formed by immersing silicon rubber molds filled with 3 mL (5×3×0.3

cm^3 molds) or 1 mL (5×1×0.2 cm^3) of the 1:1 or 1:3 mixture into a $CaCl_2$ 3 wt.% aqueous solution for 10 min. Silicon rubber molds were constructed with Ecoflex® 00-10, which is a platinum cure silicon rubber compound. It should be mentioned that the mold is not necessary for the formation of the hydrogels, which can be directly obtained by depositing the mixtures onto a cover glass or any other surface, even though it allows to control the dimensions of the hydrogel for reproducibility. Both PSS chains displaced by AA and the excess of negatively charged polymer chains were removed by thoroughly washing the samples with abundant water. Then, a blotting paper is applied to the surface of the hydrogels to remove excess water and thus prevent water leaking during measurements.

Blank samples -pure PEDOT:PSS and pure Alg hydrogels- were also fabricated for comparison purposes. While Alg hydrogels were obtained using the same procedure as before but using only the 1.3 wt% AA solution, pure PEDOT:PSS hydrogels were prepared with H_2SO_4 using the procedure described by Shi and coworkers.[14] Briefly, a PEDOT:PSS suspension (10.5 mg/mL, Clevios PH1000) containing H_2SO_4 (0.1 mol/L) was placed in a glass capillary tube and kept at 90ºC for 3h. Hydrogels for the electrochemical characterization were prepared onto an indium tin oxide (ITO)-coated polyethylene terephthalate (PET) sheet (purchased from Sigma-Aldrich).

Characterization

Attenuated total reflectance (ATR)-FTIR spectra were obtained with a FTIR 4100 spectrophotometer, equipped with a diamond crystal (Specac model MKII Golden Gate Heated Single Reflection Diamond ATR). The samples were evaluated using spectra manager software. For each sample 3 scans were performed between 4000 and 600 cm^{-1} with a resolution of 4 cm^{-1} at room temperature.

Raman spectra were acquired using a commercial Renishaw inVia Qontor confocal Raman microscope. The Raman setup consisted of two laser at 785 nm and 532 nm, both with a nominal 500 mW output power and directed through a microscope (specially adapted Leica DM2700 M microscope) to the sample, after which the scattered light is collected and directed to a spectrometer with a 1200 lines/mm grating and 2400 lines/mm grating, respectively. The exposure time was 10 s, the laser power was adjusted to 0.05% and 1%, respectively, of its nominal output power, and each spectrum was collected with three accumulations

The morphology of the prepared hydrogels was examined by scanning electron microscopy (SEM) using a Focused Ion Beam Zeiss Neon40 scanning electron microscope equipped with an energy dispersive X-ray (EDX) spectroscopy system and operating at 5 kV. All samples were sputter-coated with a thin carbon layer using a K950X Turbo Evaporator to prevent electron charging problems. Prior to SEM observation, samples were lyophilized (*i.e.* freeze-drying). The size of pores was determined from the SEM images using the software SmartTIFF (*v*1.0.1.2.).

Atomic force microscopy (AFM) images were obtained with a Molecular Imaging PicoSPM using a NanoScope IV controller under ambient conditions. The tapping mode AFM was operated at constant deflection. The row scanning frequency was set to 1 Hz. AFM measurements were performed on various parts of the films, which provided reproducible images similar to those displayed in this work. The root mean square roughness (RMS R_q), which is the average height deviation taken from the mean data plane, was determined using the statistical application of the NanoScope Analysis software (1.20, Veeco).

Measurements for water uptake were carried in distillate water. First, hydrogels were lyophilized by freeze-drying and weighted. Then, they were immersed in distilled water for 24 h (for measurements of water uptake). After that, the wet hydrogels were quickly wiped to remove the surface water with filter paper, and their weights were scored again. Water uptake was calculated as:

$$\text{Water uptake} = \frac{\mathrm{W_w} - \mathrm{W_d}}{W_d} x100\% \qquad \text{(S1)}$$

where $\mathrm{W_w}$ is the weight of the swelled hydrogel and $\mathrm{W_d}$ is the weight of the lyophilized hydrogel. Three independent measurements were carried using similar sized samples to check for reproducibility. The average values were expressed in all cases.

Transmission electron microscopy (TEM) studies were performed using a JEOL J1010 (filament: tungsten) equipped with a Gatan *Orius* 1000 slow scan *CCD* and the DigitalMicrograph (Gatan) software. The accelerating voltage was 80 kV. A Sorvall Porter-Blum microtome (Sorwall, NT, USA) equipped with a diamond knife was used to cut the sample in thin sections that were subsequently lifted onto carbon-coated grids.

The electrical conductivity was determined using a Fluke 8840A Multimeter. Measurements were performed on hydrogel samples that were prepared inside smooth rubber molds of well-defined dimensions. The latter were built using Ecoflex® 00-10 platinum cure silicone rubber compound.

Electrochemical impedance spectroscopy (EIS) diagrams were taken at open circuit (OCP) over the frequency range of 10^5 kHz to 10 Hz with potential amplitude of 0.05 V using an AUTOLAB-302N potentiostat/galvanostat. All experiments were performed at room temperature.

Electrochemical cells in three-electrode configurations were assembled for electrochemical characterization. The working consisted on the hydrogel supported by an ITO-coated PET sheet (exposed area: 1 $\mathrm{cm^2}$) while the counter electrode was platinum wire. An Ag|AgCl electrode containing saturated KCl aqueous solution (E^0 = 0.222 V *vs.* standard hydrogen electrode at 25 °C) was used as reference electrode. All electrochemical experiments were run in triplicate using a 0.1 M $CaCl_2$ solution as supporting electrolyte. The electrochemical activity was determined by cyclic voltammetry. The initial and final potentials were 0.0 V, whereas the reversal potential was 0.8 V. All measurements were performed at room temperature using a scan rate comprised between 50 and 500 mV/s. On the other hand, galvanostatic charge-discharge curves between 0.0 and 0.8 V were run at 20 $\mu A/cm^2$. All electrochemical experiments were run in triplicate with a potentiostat-galvanostat Autolab PGSTAT101 equipped with the ECD module (Ecochimie, The Netherlands).

RESULTS AND DISCUSSION

Raman spectroscopy

Raman spectra recorded for the different compositions of PEDOT/Alg-h are displayed in Figure 2b (main text). The main vibrational modes of PEDOT-h are located at 1423 cm^{-1} for the symmetric $C_\alpha=C_\beta$ stretching of the thiophene ring (the shoulder at 1488 cm^{-1} corresponds to the asymmetric $C_\alpha=C_\beta$ stretching), 1366 cm^{-1} for the $C_\beta=C_\beta$ stretching, and 1256 cm^{-1} for the inter-ring stretching vibrations.[S6,S7] Other important bands are located at 693 and 990 cm^{-1} which have been assigned to the symmetric C–S–C and oxyethylene ring respectively. Unfortunately, some of these bands overlap the most characteristic bands of Alg-h which appear at 1427 cm^{-1} for the symmetric COO-stretching bounded to Ca^{2+}, at 1301 and 1085 cm^{-1} for C–H and C–O deformations, respectively, and at 955, 886 and 811 cm^{-1} for skeletal stretching deformation and ring breathing.[S8] Instead, the asymmetric COO-stretching appears as a very weak and broad band at 1610 cm^{-1} probably due to the effect of the mass of Ca^{2+} in this mode. Although the Raman spectra of PEDOT/Alg-h prove the presence of the CP, Alg chains are practically undetectable. The Raman fingerprints of PSS phases are typically located at the vibration modes of 1000 and 1100 cm^{-1}.[S9,S10] The very low intensity of these bands is consistent with the residual presence of PSS in both PEDOT-h and PEDOT/Alg-h.

REFERENCES

S1. Gaussian 09, Revision A.02, M. J. Frisch, G. W. Trucks, H. B. Schlegel, G. E. Scuseria, M. A. Robb, J. R. Cheeseman, G. Scalmani, V. Barone, B. Mennucci, G. A. Petersson, H. Nakatsuji, M. Caricato, X. Li, H. P. Hratchian, A. F. Izmaylov, J. Bloino, G. Zheng, J. L. Sonnenberg, M. Hada, M. Ehara, K. Toyota, R. Fukuda, J. Hasegawa, M. Ishida, T. Nakajima, Y. Honda, O. Kitao, H. Nakai, T. Vreven, J. A. Jr. Montgomery, J. E. Peralta, F. Ogliaro, M. Bearpark, J. J. Heyd, E. Brothers, K. N. Kudin, V. N. Staroverov, R. Kobayashi, J. Normand, K. Raghavachari, A. Rendell, J. C. Burant, S. S. Iyengar, J. Tomasi, M. Cossi, N. Rega, J. M. Millam, M. Klene, J. E. Knox, J. B. Cross, V. Bakken, C. Adamo, J. Jaramillo, R. Gomperts, R. E. Stratmann, O. Yazyev, A. J. Austin, R. Cammi, C. Pomelli, J. W. Ochterski, R. L. Martin, K. Morokuma, V. G. Zakrzewski, G. A. Voth, P. Salvador, J. J. Dannenberg, S. Dapprich, A. D. Daniels, Ö. Farkas, J. B. Foresman, J. V. Ortiz, J. Cioslowski and D. J. Fox, Gaussian, Inc., Wallingford CT, 2009.

S2. Y. Zhao and D. G. Truhlar, *J. Chem. Phys,*. 2006, **125**, 194101.

S3. Y. Zhao and D. G. Truhlar, *Theor. Chem. Acc.*, 2008, **120**, 215−241.

S4. S. Miertus, E. Scrocco and J. Tomasi, *Chem. Phys.*, 1981, **55**, 117-129.

S5. S. Miertus and J. Tomasi, *Chem. Phys.*, 1982, **65**, 239-245.

S6. Y.-K. Han, M.-Y. Chang, W.-Y. Huang, H.-Y. Pan, K.-S. Ho, T.-H. Hsieh and S.-Y. Pan, *J. Electrochem. Soc.*, 2011, **158**, K88-K93.

S7. A. A. Farah, S. A. Rutledge, A. Schaarschmidt, R. Lai, J. P. Freedman and A. S. Helmy, *J. Appl. Phys.*, 2012, **112**, 113709.

S8. S. Koburger, A. Bannerman, L. M. Grover, F. A. Müller, J. Bowen and J. Z. Paxton, *Biomater. Sci.*, 2014, **2**, 41-51.

S9. B. Sun, Z. Wang, Q. He, W. Fan and S. Cai, ***Soft Matter***, 2017, **13**, 6852-6857.

S10. X.-N. Shi, W.-B. Wang and A.-Q. Wang, Colloids Surf *B Biointerfaces,* 2011, **88**, 279- 286.

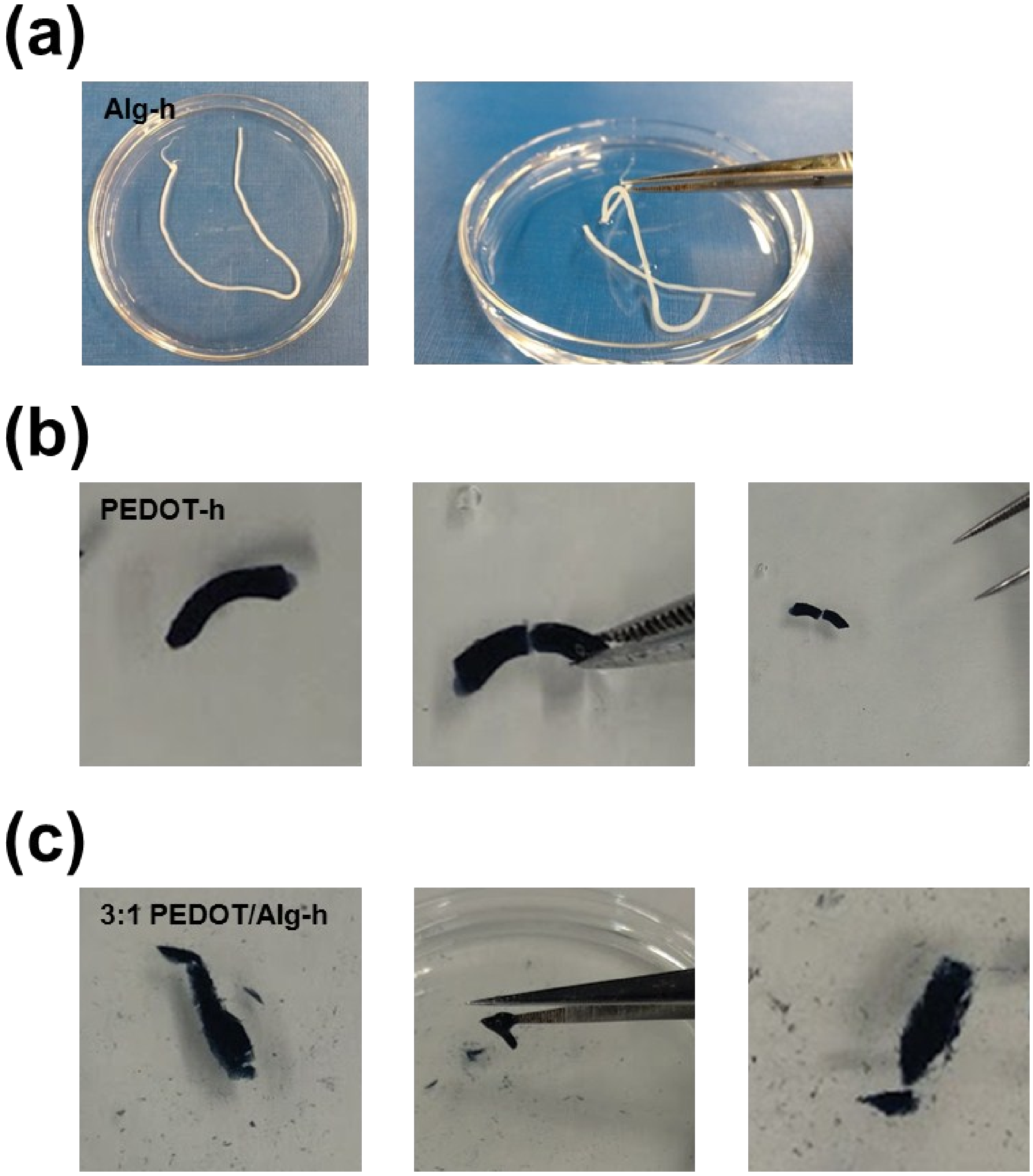

Figure S1. Photographic images of (a) Alg-h, (b) PEDOT-h and (c) 3:1 PEDOT/Alg-h as prepared, handled with tweezers and, for both PEDOT-h and 3:1 PEDOT/Alg-h, the hydrogel broken after this operation due to its own weight.

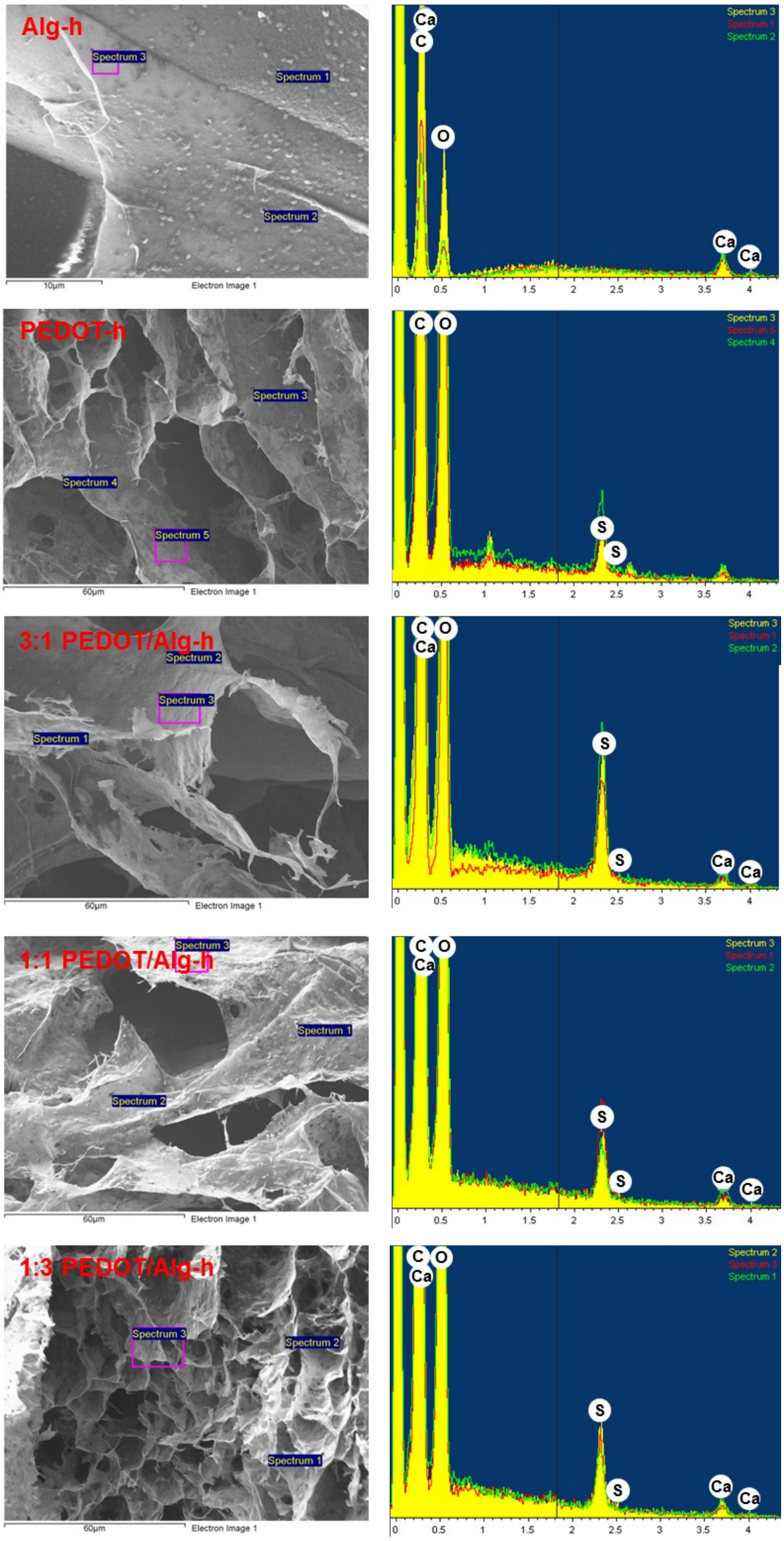

Figure S2. SEM micrograph (left) and EDX spectra (right) of Alg-h, PEDOT-h and 3:1, 1:1 and 1:3 PEDOT/Alg-h.

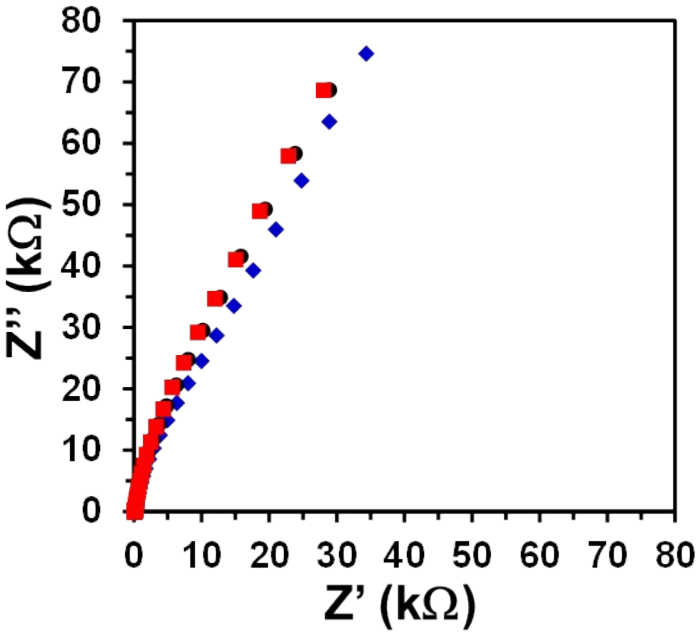

Figure S3. Nyquist plots recorded for 1:3 PEDOT/Alg-h.

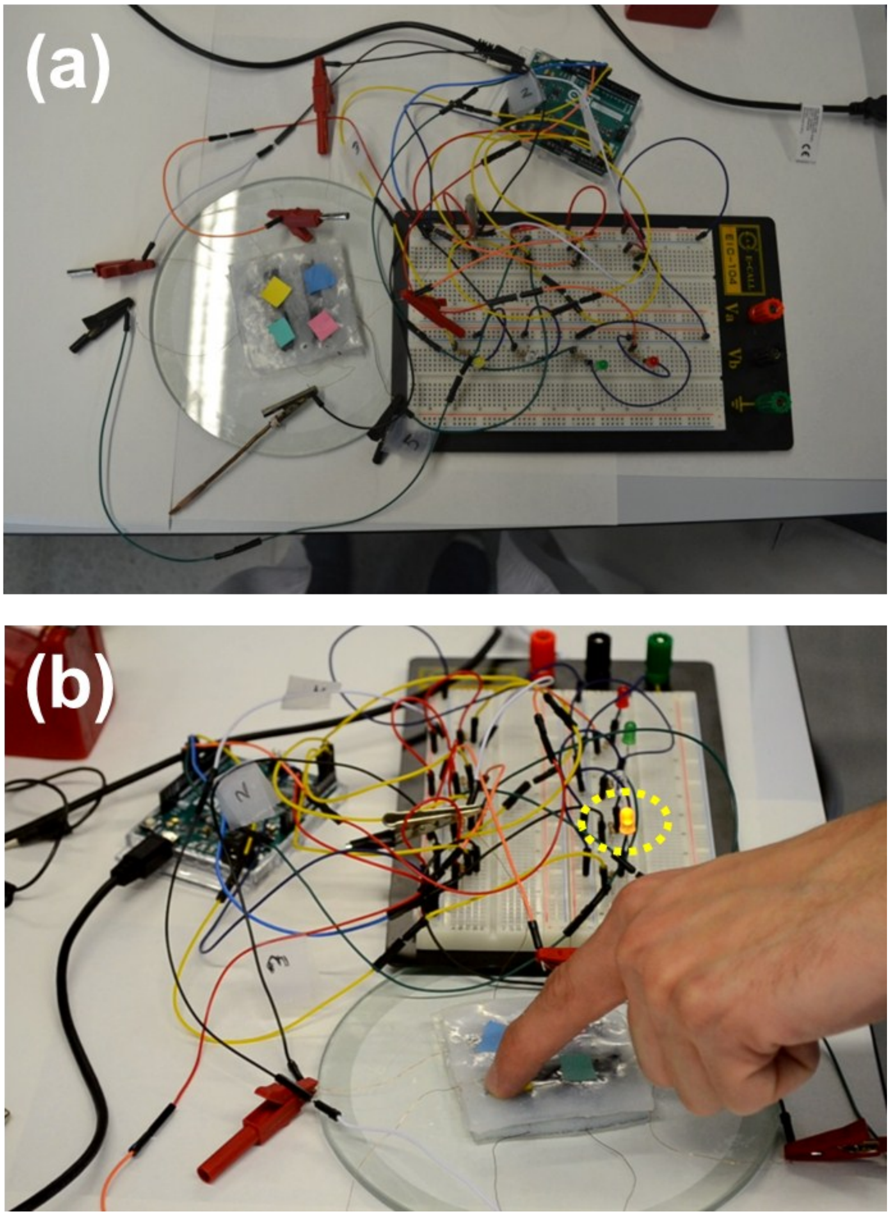

Figure S4. Demonstration of the sensing capacity of the reprocessed tactile pressure sensor array in terms of location and pressure of touches: (a) voltage divider device constructed using the reprocessed sensor array; and (b) demonstration of the sensing capacity of the reprocessed sensor array.